 doi:10.20944/preprints201812.0252.v1

Article

The influence of the post weld heat treatment on the microstructure of Inconel 625/carbon steel bimetal joint obtained by explosive welding

Robert Kosturek [1], Marcin Wachowski [1,*], Lucjan Śnieżek [1], Michał Gloc [2]

[1] Military University of Technology, Faculty of Mechanical Engineering, 2 gen. W. Urbanowicza str., 00-908 Warsaw, Poland
[2] Warsaw University of Technology, Faculty of Materials Science and Engineering, 141 Woloska str., 02-507 Warsaw, Poland
* Correspondence: marcin.wachowski@wat.edu.pl; Tel.: +48-261-839-245

Abstract: In this investigation steel P355NH has been successfully cladded with Inconel 625 through the method of explosive welding. Explosively welded bimetal clad-plate was subjected to the two separated post weld heat treatment processes: stress relief annealing (at 620°C for 90 minutes) and normalizing (at 910°C for 30 minutes). In order to analyze the microstructure of the joint in the as-welded state and to investigate the influence of the post weld heat treatment on it, the light and scanning electron microscope observations and microhardness analysis have been performed. The examination of the diffusion zone microstructure has been performed by using the scanning transmission electron microscope. It was stated that obtained joint has characteristic wavy-shape geometry with the presence of the melted zones and severe deformed grains of both joined materials. Strain hardening of the materials in joint zone was established with microhardness analysis. In both of the heat treatments the changes in the grain structure have been observed. The normalizing heat treatment has the most significant impact on the microstructure of the joint as well as the concentration of the chemical elements in the joint zone. It was reported that due to normalizing the diffusion zone has been formed together with precipitates in the joint zone. The analysis of the diffusion zone images leads to the conclusion that the diffusion of alloying elements from Inconel 625 to steel P355NH takes place along the grain boundaries with additional formation of the voids in this area. The precipitates in Inconel 625 in the joint zone are two type of carbides – chromium-rich and molybdenum-rich. Scanning transmission electron microscope observation of the grain microstructure in the diffusion zone shows that this area consists of equiaxed grains (from the side of Inconel 625 alloy) and columnar grains (from the side of steel P355NH).

Keywords: explosive welding; heat treatment; Inconel; steel; microstructure.

1. Introduction

Corrosive wear is a significant problem for the utilization of components of equipment operating in an aggressive environment, such as reactors, tanks, heat exchangers and pipelines in the chemical industry and geothermal power plants [1, 2]. The use of corrosion resistant alloys for the manufacture of these components is generally associated with considerable costs. An economical solution is to use clad materials where relatively inexpensive material, such as carbon steel, is covered by a layer of material that will provide protection from corrosion, e.g. acid resistant steel, which significantly reduces the costs of material used for the production of the equipment [3-5]. This paper investigates steel P355NH cladded with Inconel 625 as bimetallic material of the above type. Steel P355NH, weldable constructional steel with fine grain microstructure, is used as material for the manufacture of pressure equipment operating under high temperature (up to 450°C) [6]. The poor corrosion resistance of this steel limits its applications as a construction material for the equipment working in

 doi:10.20944/preprints201812.0252.v1

the aggressive environment significantly. The potential solution of this problem is cladding steel P355NH with a layer of Inconel 625, high-temperature creep resistant alloy of nickel and chromium with an additive of molybdenum and niobium which is characterized by high resistance to oxidizing and reducing environment as well as pitting and crevice corrosion and it also displays tolerance to a wide range of the operating temperature (from -150°C to 982°C) [7]. Cladding of the materials or modifying their surface layer are widely used technologies in the production of industry equipment and machinery, but not all of this process can provide sufficient properties in terms of cladded material formability [8-10]. The manufacturing of clad material in which steel P355NH plays the load-bearing role and a layer of Inconel 625 alloy provides protection from corrosion may be achieved through explosive welding [11-14]. In this process, the energy released during detonation of the high explosive is used to accelerate one metal plate into another, and as the consequence the high velocity collision of metal plates occurs [15,16]. The result of this high energy collision is bringing the surfaces of the welded materials close enough to each other to obtain interaction between their atoms and the consequent formation of a metallic bond between them [14, 18-20]. The severe plastic deformation of the materials significantly influences the microstructure of the materials and causes strain hardening in the joint zone. Clad-plates manufactured by this method are subjected to further technological processes to form specific equipment components for the industry, e.g. pipes, pressure vessels, tube plates for heat exchangers. In order to decrease the degree of strain hardening of the materials and reduce the residual stresses, the clad-plates are subjected to heat treatment [21-23]. The annealing of bimetallic materials in many cases leads to microstructural changes within the joint zone, which may deteriorate the mechanical properties of clad-plate [24]. Steel clad with Inconel 625 using explosive welding has been the subject of numerous studies, which have confirmed that it is possible to obtain such a bimetallic joint through explosive welding [11-14]. However, literature does not contain sufficient investigation of the effect of heat treatment on structural changes in the joint. According to previous studies performed by the authors of this paper, the normalizing of Inconel 625 – steel P355NH joint obtained by explosive welding decreases its shear strength by 33% (decrease from 572 MPa to 383 MPa, determined according to PN-EN13445:2014) [22]. The present paper aims to investigate the causes of such a drastic reduction in the strength of the joint. Structural changes may involve both evolution of the grainy structure of the materials and diffusion processes within the joint [16, 21, 25-28]. Depending on the mutual solubility of the diffusing chemical elements of the alloy, brittle intermetallic compounds or new solid solutions may be formed in the joint area [29, 30]. The Kirkendall effect may occur as the result of the diffusion changes and leads to formation of voids in the joint area due to differences in diffusion rates of specific alloying elements of the welded materials [25, 27, 31-33]. Additionally, Inconel alloys show a tendency to form precipitates (e.g. carbides, γ', γ'' and δ phases) during long-term exposure to high temperature [34-37]. Importantly, plastic deformation of Inconel alloys exerts a considerable impact on the kinetics of precipitate formation, as it promotes their quicker development [38-40]. Another factor promoting formation of carbides is heat treatment-induced diffusion of carbon from the steel to the Inconel alloy, which contains elements showing considerable affinity to carbon (Cr, Mo, Nb) [41]. For this reason, the layer of Inconel 625 alloy in the area of the joint produced through explosive welding is a zone with potential to formation of precipitates during heat treatment of the investigated bimetal clad-plate.

2. Materials and Methods

The materials used in the study included a plate of steel P355NH of 10 mm thickness and a sheet of Inconel 625 alloy of 3 mm thickness. The chemical composition of the materials is presented in Table 1 (Table 1). Samples were cut out of the workpieces to investigate the microstructure of the materials in the as-received state. The process of explosive welding of steel P355NH and Inconel 625 alloy was performed by EXPLOMET High-Energy Techniques Works company. The explosive was modified ammonium nitrate fuel oil (ANFO), with detonation velocity of 2700 m/s, determined using optical fiber sensors. Three samples were cut out of the bimetallic clad-plate produced by explosive welding, as shown on Figure 1.

Preprints (www.preprints.org) | NOT PEER-REVIEWED | Posted: 20 December 2018 doi:10.20944/preprints201812.0252.v1

Table 1. Chemical composition of the alloys to be joined [% mass]

Inconel 625	Al	Cr	Fe	Mo	Nb	Ti	Ni
	0.16	21.5	4.6	8.7	3.32	0.18	Base
St. P355NH	C	Cr	Si	Mn	Ni	Cu	Fe
	0.18	0.02	0.35	1.19	0.22	0.2	Base

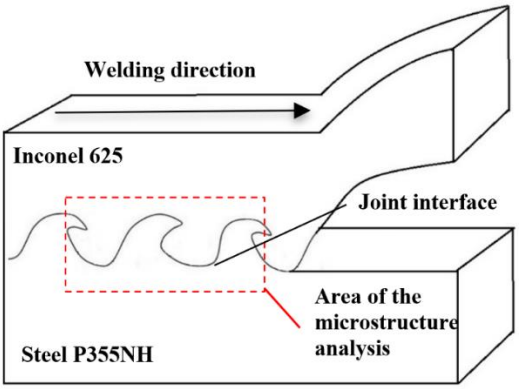

Figure 1. Area from which samples of bimetallic clad-plate were collected for microstructure investigation.

One of the samples was subjected to heat treatment of stress relief annealing (at 620°C for 90 minutes), and another to normalizing (at 910°C for 30 minutes). The parameters of the post weld heat treatment processes were selected by EXPLOMET company based on their many years of experience in the heat treatment of clad materials. As a result, three samples were obtained: a sample after explosive welding, sample after post weld stress relief annealing and sample after post weld normalizing (Table 2).

Table 2. Samples designation

Designation	Description
InSt EXW	Bimetallic joint Inconel 625/ steel P355NH in the as-welded state
InSt HTR	Bimetallic joint Inconel 625/ steel P355NH after stress-relief annealing (620°C / 90min)
InSt HTN	Bimetallic joint Inconel 625/ steel P355NH after normalizing (910°C / 30min)

The samples were mounted in resin, grinded with abrasive paper of 80, 320, 600, 1200 and 2400 gradations and polished using diamond paste of 1 μm gradation. To reveal the microstructure of steel P355NH, 2% nital with etching time of 5-10 seconds was used and for Inconel 625 alloy, acetic glyceregia (15 ml HCl 38%, 10 ml of acetic acid 99%, 5 ml HNO3 65%, 1-2 drops of glycerol) with etching time of 15 minutes. The microstructure of the samples was investigated using light microscope LEXT OLS 4100 and scanning electron microscope Joel JSM 6610. Additionally, an analysis of the microstructure of the joint zone was performed in the sample InSt HTN using scanning transmission electron microscope (STEM) Hitachi S-5500N. The samples for STEM were prepared using Dual beam system Hitachi NB-5000. The Vickers microhardness test was performed with loading of 100g. Microhardness distributions were prepared for each sample. The first two measurements were performed 200 μm from the joint line, in the layer of Inconel 625 alloy and in steel P355NH. Subsequently, measurement imprints were guided towards the edge of the samples, at the distance of 2000 μm.

Preprints (www.preprints.org) | NOT PEER-REVIEWED | Posted: 20 December 2018 doi:10.20944/preprints201812.0252.v1

3. Results

3.1. Microstructure of the raw materials

Microstructures of steel P355NH (Figure 2a) and Inconel 625 alloy (Figure 2b) in the as-received state are presented on Figure 2. Steel P355NH shows ferrite-pearlite microstructure with banded distribution of the pearlite, typical for plates after rolling process. According to the measurements, it is characterised by the presence of fine equiaxial grains sized 15.5 ± 4.1 μm, specific to steel after normalizing. The microstructure of Inconel 625 alloy is more heterogeneous, with visible twins and grains sized 49.4 ± 15.6 μm. The measurement outcomes for microhardness in the as-received state were 249.6± 16.3 HV0.1 for Inconel 625 alloy and 150.6 ± 4.9 HV0.1 for steel P355NH, respectively.

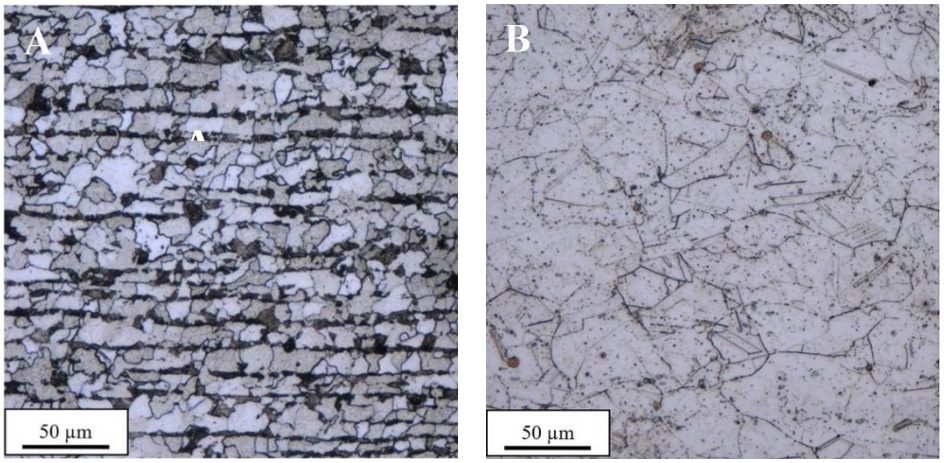

Figure 2. Microstructure of materials in the as-received state a) steel P355NH b) Inconel 625.

3.2. Microstructure of the raw materials

The joint produced by explosive welding shows a characteristic wavy geometry. The grains in the joint zone have undergone severe plastic deformation and have been observed to wrap to areas of intersurface waves in the samples after etching of steel P355NH (Figure 3a) and Inconel 625 alloy (Figure 3b).

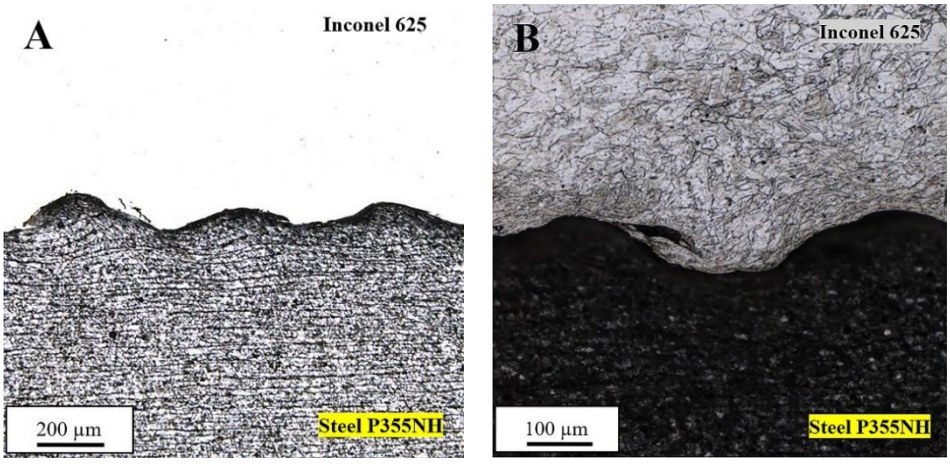

Figure 3. Microstructure of the joint in InSt EXW sample: (a) after etching of steel P355NH; (b) after etching of Inconel 625 alloy.

It has been reported that the microstructure of steel P355NH close to the joint line consist of ultrafine grains of 1-2 μm size (Figure 4). Deformation texture of the grains were not observed and their ultrafine size was a results of dynamic recrystallization process. It is well known

Preprints (www.preprints.org) | NOT PEER-REVIEWED | Posted: 20 December 2018 doi:10.20944/preprints201812.0252.v1

phenomenon that due to severe and dynamic plastic deformation the metallic material can undergo dynamic recrystallization. In this case the ultrafine grains of steel P355NH have been found on the joint line where the most severe plastic deformation occurs during explosive welding process. Beneath dynamic recrystallized grains it can be observed the occurrence of elongated, compressed grains with their elongation according to the direction of detonation (welding).

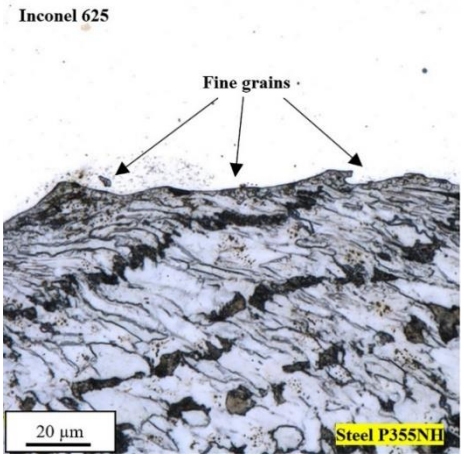

Figure 4. Ultrafine grain microstructure of steel P355NH in the joint area.

The observation using scanning electron microscope showed the occurrence of melted zones in the joint, where the two welded materials blended (Figure 5a). In the melted zones, the investigation revealed the presence of joint imperfections in the form of both cracks and fragments of the surface layer of steel P355NH, which underwent partial fragmentation during explosive welding process, as evidenced by linear analysis of the chemical composition (Figure 5b) and analysis of iron (Figure 5c) and nickel (Figure 5d) distribution at the sample surface (mapping). The results of the melted zone chemical composition investigation indicate on the highest participation of Inconel 625 alloying elements in this area with small fluctuations near to the steel P355NH fragment. It can be observed on Figure 5c and Figure 5d that despite the significant concentration of steel fragments in the melted zone presence of Inconel 625 alloy fragments has not been reported. It can be related with higher tendency to fragmentation of the base-plate material in the explosive welding system or with higher coherency of Inconel 625 alloy during high velocity collision of bonding process.

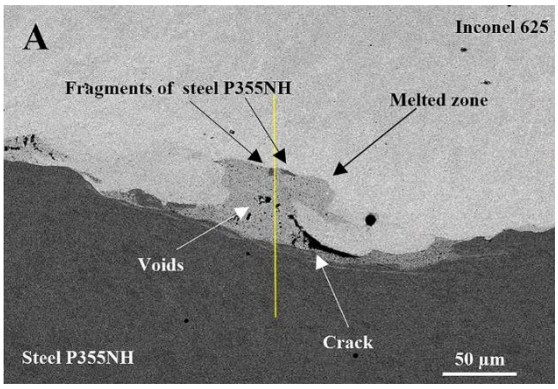

Preprints (www.preprints.org) | NOT PEER-REVIEWED | Posted: 20 December 2018 doi:10.20944/preprints201812.0252.v1

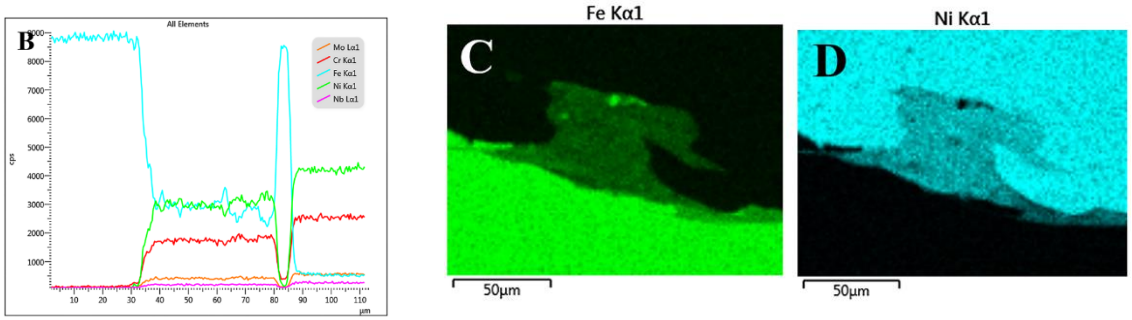

Figure 5. Melted zone in InSt EXW sample: (**a**) with linear analysis of the chemical composition; (**b**) (yellow marker) and mapping of iron (**c**) and nickel (**d**).

3.3. Microstructure of InSt HTR joint

Post weld stress relief annealing of the Inconel 625/ steel P355NH bimetallic clad-plate, performed at 620°C for 90 minutes influence slightly the microstructure of the joint zone. The partial recrystallization of steel P355NH microstructure has been reported in the area of 20 – 30 μm from the joint line (Figure 6a). New, equiaxial grains formed on the joint line do not have deformation texture of previous compressed, elongated grains. The microstructure of steel P355NH farther from the joint line (about 30 μm) maintains the deformation texture and no recrystallized grains have been observed. On the other hand, the microstructure of Inconel 625 alloy did not reveal visible changes in the grain morphology after stress relief annealing compared to its microstructure in the as-welded state (Figure 6b).

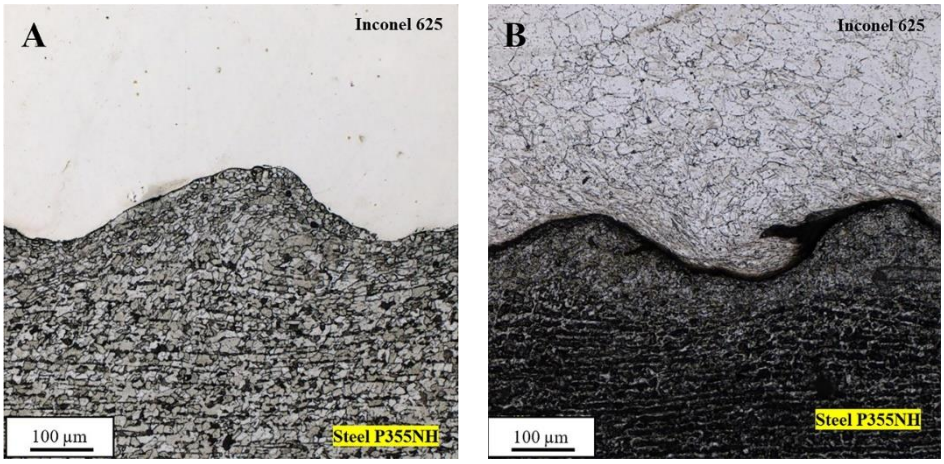

Figure 6. Microstructure of the joint in InSt HTR sample: (**a**) after etching of steel P355NH; (**b**) after etching of Inconel 625 alloy.

The scanning electron microscope observations did not show any visible changes in the concentration of the alloying elements in the joint zone (Figure 7). Both the bound between joined materials and melted zone are not affected by stress relief annealing in terms of chemical composition. The small imperfections in form of voids are possible to observe in melted zone, which is localized at the side of one of the intersurface wave.

Preprints (www.preprints.org) | NOT PEER-REVIEWED | Posted: 20 December 2018 doi:10.20944/preprints201812.0252.v1

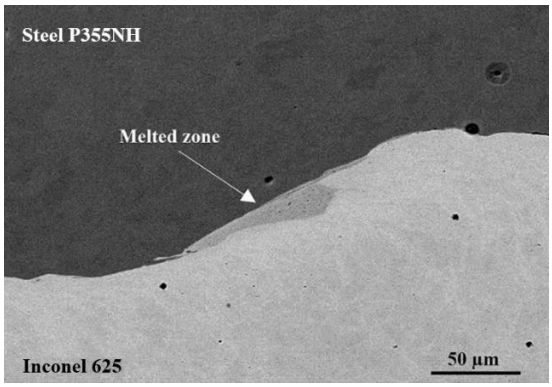

Figure 7. Image of the joint in InSt HTR sample from the scanning electron microscope.

3.4. Microstructure of InSt HTN joint

The microstructure of the joint subjected to normalizing at 910°C for 30 minutes changed significantly. It has been reported that due to this post weld heat treatment the complete recrystallization of microstructure of both joined materials – steel P355NH (Figure 8a) and Inconel 625 (Figure 8b) occurs. The welded materials have microstructures consist of fine, equiaxial grains and no deformation texture is noticeable. The size of steel grains is about 20 µm, which is a typical value for this material after normalizing. Additionally, it has been observed the presence of ultrafine grains with size about 5 µm of steel P355NH on the joint line (Figure 8a). In case of Inconel 625 grains have size also about 20 µm with low participation of twins and significant amount of the precipitates localized on the grain boundaries. Similarly, it has been noticed that grains of Inconel 625 close to the joint line are ultrafine with their size equal to 3-5 µm.

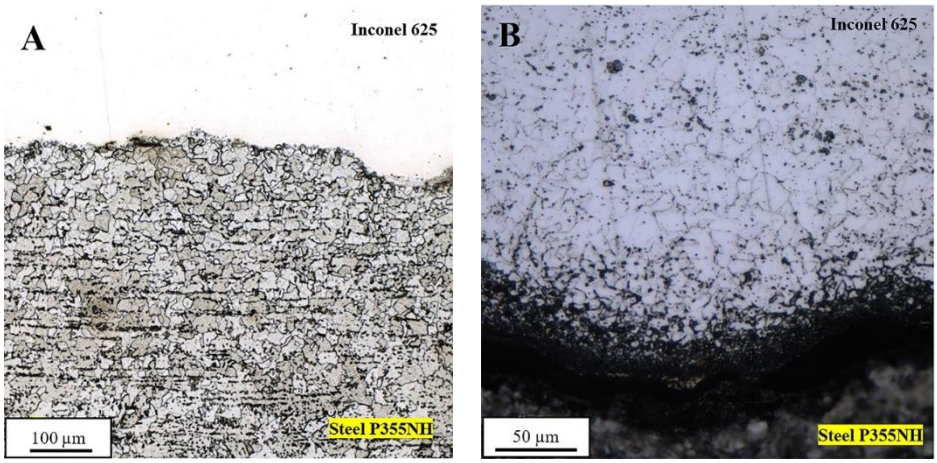

Figure 8. Microstructure of the joint in InSt HTN sample: (**a**) after etching of steel P355NH (**b**) after etching of Inconel 625 alloy.

The observation using scanning electron microscope showed significant changes in the concentration of alloying elements in the joint area. It has been stated that alloying elements of Inconel 625 were found to diffuse into steel P355NH along the grain boundaries (Figure 9a). Additionally, voids were found in the diffusion zone localized mainly on the grain boundaries and on the joint line (Figure 9b). The voids founded in the diffusion zone are mainly concentrated on the side of Inconel 625 alloy. Another noticeable change compared to the joint in the as-welded state is formation of precipitates in the joint zone, which are localized in Inconel 625 alloy (Figure 9a). Scanning electron microscope observations revealed the presence of two types of precipitates in Inconel 625 alloy – light precipitates (suggesting a high concentration of alloy elements heavier than nickel) and dark precipitates (high concentration of alloying elements lighter than nickel).

Preprints (www.preprints.org) | NOT PEER-REVIEWED | Posted: 20 December 2018 doi:10.20944/preprints201812.0252.v1

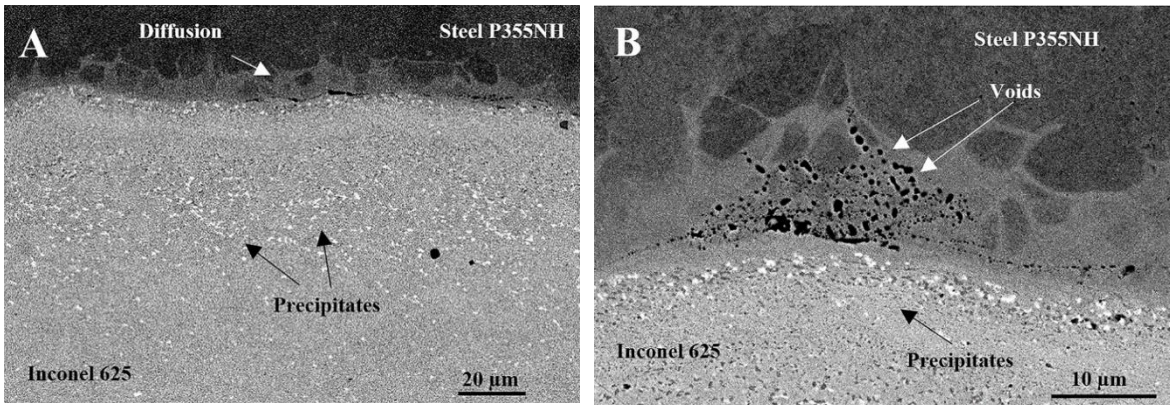

Figure 9. Image of the joint in InSt HTN sample from the scanning electron microscope: (**a**) diffusion of alloying elements through the joint line and precipitates in Inconel 625 alloy; (**b**) diffusion zone with visible voids along the grain boundaries and the joint line.

The results of an analysis of alloying elements distribution on the surface of the sample in the joint area indicate an increased concentration of chromium in dark precipitates (Figure 10b) and an elevated concentration of molybdenum in light precipitates (Figure 10c). The results of nickel (Figure 10a) and iron (Figure 10d) distributions in the joint allow to observe a formed diffusion zone and estimate deep of alloying elements diffusion through the joint line. It has been stated that diffusion of Inconel 625 main alloying elements – nickel and chromium is about 40 µm, what determines the width of diffusion zone. On the other hand, the diffusion of iron from steel P355NH into Inconel 625 alloy was found up to 5 µm deep.

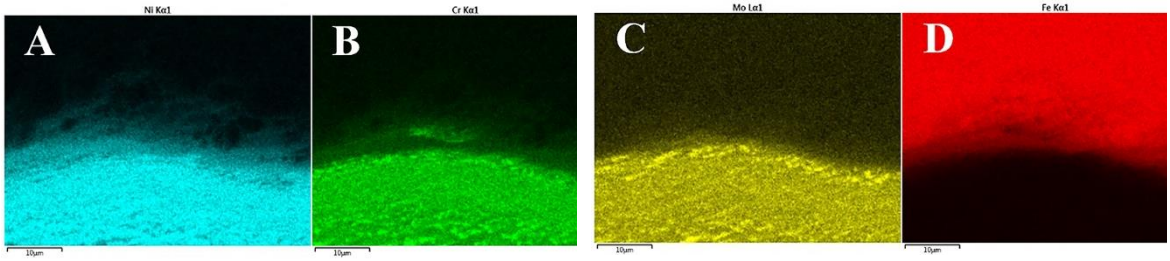

Figure 10. Distribution of alloying elements on the surface of InSt HTN sample in the joint area: (**a**) nickel; (**b**) chromium; (**c**) molybdenum and (**d**) iron.

3.5. Scanning transmission electron microscope observations of the diffusion zone

Observations of the diffusion zone performed on scanning transmission electron microscope allow to investigate the grain microstructure of this area. It has been stated that in terms of grain structure the diffusion zone consists of two subzones: area of equiaxed grains (from side of Inconel 625 alloy) and area of columnar grains (from side of steel P355NH) (Figure 11a). In both cases the microstructure consists of ultrafine grains with their size within the range of 400nm – 1µm. Predominantly, the finer grains close to Inconel 625 are equiaxed and columnar grains close to P355NH have slightly larger size. Additionally, it has been reported the occurrence of precipitates with their width about 50 nm in the diffusion zone (Figure 11b).

Preprints (www.preprints.org) | NOT PEER-REVIEWED | Posted: 20 December 2018 doi:10.20944/preprints201812.0252.v1

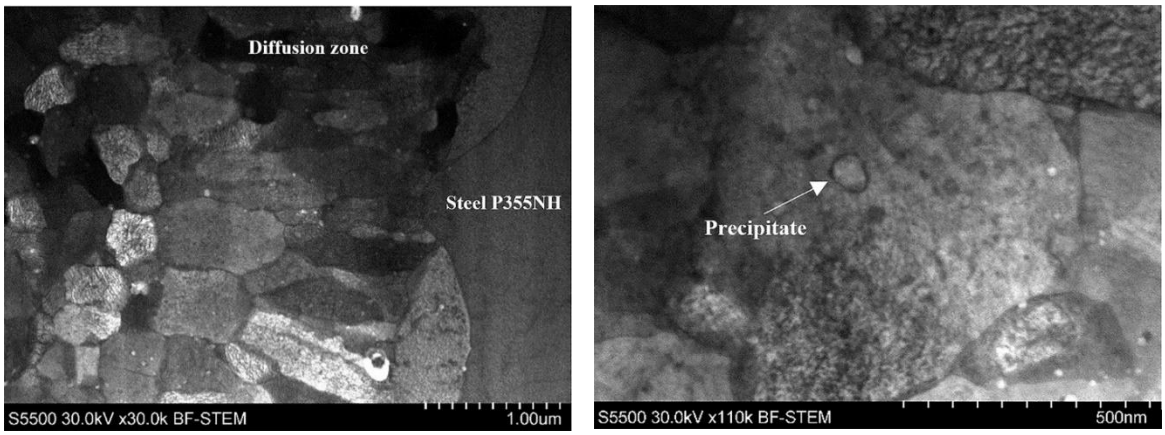

Figure. 11. Image of the grain microstructure of the diffusion zone in InSt HTN sample (**a**); Image of the precipitate in the diffusion zone (**b**).

The linear analysis of chemical composition has been performed in order to investigate subzone of columnar grains (Figure 12). Results indicate on similar concentration of chromium and niobium in the analyzed area. On the other hand the elements such as iron and nickel, which are main components of the diffusion zone, show significant fluctuations in their concentration in this zone. It has been reported that concentration of nickel decreases drastically on the border between columnar grains area of the diffusion zone and steel P355NH. At the same time the concentration of iron increases, also rapidly. This results of linear analysis together with scanning transmission electron microscopy observations of this area suggest the predominate role of nickel and iron concentration ratio in the forming of diffusion zone. The precipitates founded in this area were a subject of further investigation and observations performed on scanning transmission electron microscope reveal their specific structure consisted of core and shell (Figure 11 b). In order to examine chemical composition of precipitate in the diffusion zone the linear analysis was performed (Figure 13). The shell-core structure has been confirmed in terms of chemical composition, since it has been reported that in the precipitate area there are significant differences in distribution of alloying elements. Its shell has highest concentration of niobium and molybdenum, while core consists of chromium and also of niobium and molybdenum (compared to the average value of concentration of this elements in the diffusion zone).

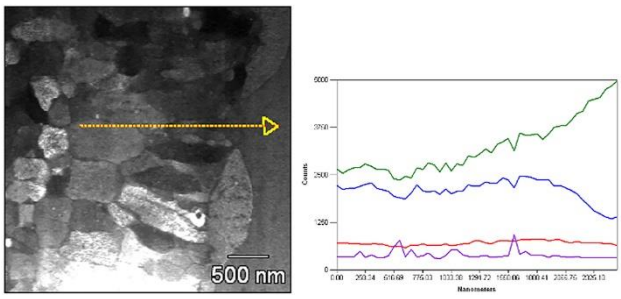

Figure. 12. The results of linear analysis of the chemical composition of columnar grains in the diffusion zone. Lines designation: Fe (green), Ni (blue), Cr (red), Nb (purple).

Preprints (www.preprints.org) | NOT PEER-REVIEWED | Posted: 20 December 2018 doi:10.20944/preprints201812.0252.v1

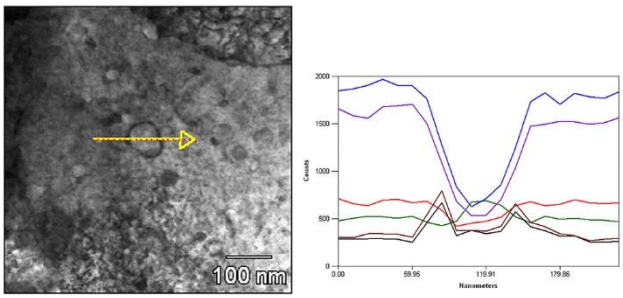

Figure. 13. The results of linear analysis of the precipitate in the diffusion zone. Lines designation: Fe (blue), Ni (purple), Cr (green), Nb (black), Mo (burgundy), C (red).

3.6. Microhardness analysis

The influence of the explosive welding process on the joined materials in terms of strain hardening was established by microhardness analysis (Figure 14). The highest degree of strain hardening has been revealed close to the joint line, where welded materials were subjected to the severest plastic deformation due to high velocity collision during explosive welding process. In this area, the microhardness of Inconel 625 alloy increased by ca. 200 HV and in case of steel P355NH by ca. 100 HV. A noteworthy finding is that hardening of steel P355NH in the joint shows a homogeneous nature, while in Inconel 625 alloy microhardness decreased with increasing distance from the joint. Stress relief annealing reduced the microhardness of steel P355NH by ca. 40 HV and led to a monotonic decrease in the microhardness of Inconel 625 alloy. It is mostly related to recrystallization of steel P355NH grains and presumably the decreasing of the residual stress of the welded materials in the joint zone. The post weld heat treatment in the form of normalizing reduced the microhardness of steel P355NH and Inconel 625 to their baseline value, measured in the as-received state.

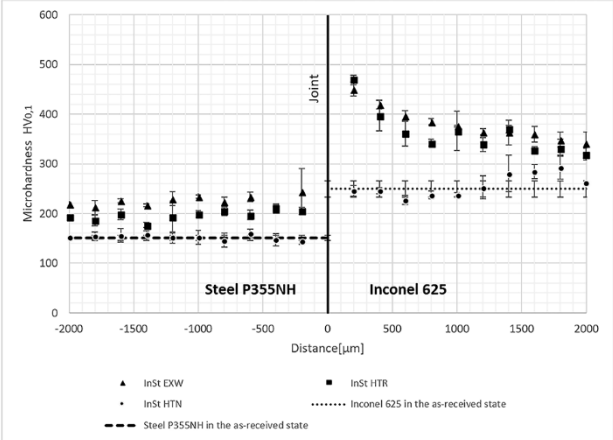

Figure 14. The results of microhardness analysis.

4. Discussion

The technique of explosive welding has produced a high quality joint between steel P355NH and Inconel 625 alloy, with characteristic wavy geometry and small amount of imperfections in the form of cracks, voids and melted zones. The melted zones have been found to contain evenly participation of welded materials which were mixed in this area. Additionally it has been reported that melted zones have an increased concentration of imperfections (voids and cracks) as well as they contain fragments of steel P355NH surface layer. Light microscope observation of the bimetal microstructure after etching of steel P355NH and Inconel 625 alloy has revealed severe plastic deformation of the materials in the joint area. Elongated, compressed grains wrapping into

Preprints (www.preprints.org) | NOT PEER-REVIEWED | Posted: 20 December 2018 doi:10.20944/preprints201812.0252.v1

intersurface waves have been found. Plastic deformation of the welded materials has been also reflected in the results of microhardness analysis, which indicate on significant strain hardening of steel P355NH and Inconel 625 alloy in the joint area. The microstructure of steel P355NH has shown ultrafine with their size about 1μm, dynamically recrystallized grains localized on the joint line. Heat treatment, both in the form of stress relief annealing and normalizing, has resulted in recrystallisation of steel P355NH grains in the joint area. The steel grains are finest at the joint line, which indicates on cumulation of the highest deformation level in this area due to interaction of the welded materials during collision. This finding is confirmed by the analysis of heat-activated phenomena as a function of the temperatures used for heat treatment. As a result of stress relief annealing at 620°C, recrystallisation was found only in the joint area, while the banded grainy structure of the steel at a distance of ca. 100μm from the joint continued to show the original banded morphology. On the other hand, an increase of annealing temperature to 910°C results in a complete restructure of the grainy microstructure of steel P355NH, which had been defected through severe plastic deformation due to explosive welding process. It is a well known fact that the higher degree of plastic deformation, the lower energy is necessary to initiate and complete heat-activated phenomena and therefore the recrystallisation temperature is lower, which explains the incomplete restructure of the deformed steel structure after stress relief annealing. Changes in the concentration of alloying elements in the joint area after heat treatment in the form of normalizing are manifested through formation of both a diffusion zone and precipitates in Inconel 625 alloy. An analysis of images of the diffusion zone by scanning electron microscope leads to the conclusion that the diffusion of alloying elements of Inconel 625 alloy into steel P355NH takes place along the grain boundaries. Moreover, voids have been found in the diffusion zone, which are most probably due to the Kirkendall effect. An analysis of the phase equilibrium of iron-nickel may suggest that the diffusion zone is composed predominantly of nickel austenite γ and a small amount of nickel ferrite α (Figure 15).

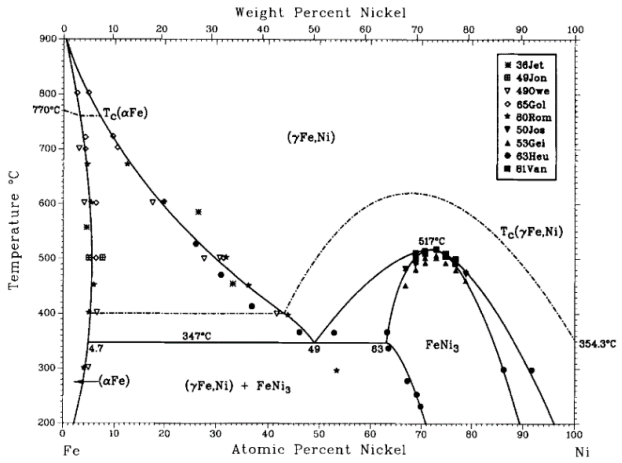

Figure 15. Graph of phase equilibrium for iron – nickel [42].

Precipitates which formed due to normalizing in Inconel 625 alloy are located along the grain boundaries and twins, which has been revealed based on comparison of images of the sample after etching from the scanning electron microscope and light microscope. An analysis of an isothermal transformation diagram for Inconel 625 alloy leads to the conclusion that the parameters of the normalizing used are close to the area of carbide formation, mainly of MC and M_6C type (Figure 16).

Preprints (www.preprints.org) | NOT PEER-REVIEWED | Posted: 20 December 2018 doi:10.20944/preprints201812.0252.v1

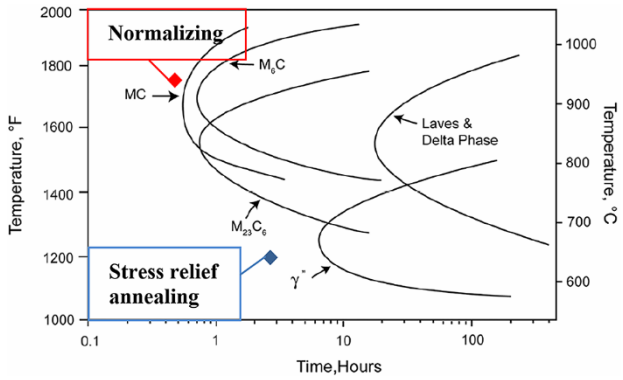

Figure 16. Isothermal transformation diagram for Inconel 625 alloy [35]. Values of stress relief annealing and normalizing have been marked.

A noteworthy fact is that the severe plastic deformation of Inconel 625 alloy in the joint reduced the energy of heat-activated processes, including precipitate processes. An additional factor promoting formation of carbides is diffusion of alloying elements of steel P355NH into Inconel 625 alloy (in particular carbon, whose content in the steel P355NH is about 0.18%). An analysis of distribution of alloying elements on the surface of the sample and microstructure observations using the scanning electron microscope enabled identifying two basic types of precipitates: light precipitates, rich in molybdenum, and dark precipitates, rich in chromium. Literature on diffusion in the bimetallic configuration of Inconel 625 alloy and low-alloyed steel precisely describes the precipitates as carbides of M_6C type in the case of high molybdenum content and of $M_{23}C_6$ type in the case of high chromium content [41]. The structural analysis of samples after normalizing indicates that both the diffusion zone and precipitates in Inconel 625 alloy represent the causes of deteriorated endurance of the joint compared to the as-welded state. In the diffusion zone, not only voids have been found, but also the microstructure itself, which contains soft nickel ferrite α on the side of steel P355NH and resistant nickel austenite γ on the side of Inconel 625 alloy, causes the significant decrease in the strength of the bond between the welded materials. Carbides, forming along the grain boundaries and twins in Inconel 625 alloy, also reduce the coherence of the material in the most crucial zone, i.e. the joint. The results of scanning transmission electron microscope observations of the diffusion zone, allow to investigate the microstructure of the diffusion zone, which consist of equiaxed and columnar grains. The precipitates in the diffusion zone with size about 50 nm are chromium-rich, surrounded by area of high concentration of niobium and molybdenum, what together with scanning transmission electron microscopy observations suggest the shell-core structure.

5. Conclusions

Analysis of Inconel 625/steel P355NH joint microstructure in the as-welded state and after two different, separated types of heat treatment (stress relief annealing and normalizing) allowed the following conclusions to be drawn.

1. The process of explosive welding using ammonium nitrate (V) as the explosive, with detonation speed of ca. 2700m/s allowed to obtain joint between steel P355NH and Inconel 625 alloy. The wavy-shape joint was found to include melted zones with an increased concentration of imperfections in the form of cracks, voids and fragments of the surface layer of steel P355NH.
2. Stress relief annealing (620°C / 90 min) led to partial recrystallization of steel P355NH in the joint area. At the same time no changes in the grainy microstructure of Inconel 625 and chemical composition of the joint have been noticed.

3. Heat treatment in the form of normalizing (910°C/ 30 min) resulted in complete recrystallization of both welded materials, which was additionally confirmed by distributions of microhardness.
4. Diffusion zone of ca. 20 μm thickness formed in the joint due to normalizing. Diffusion of Inconel 625 alloying elements into steel P355NH took place along the grain boundaries. Moreover, voids have been found in the diffusion zone, which are most probably due to the Kirkendall effect.
5. It has been reported the presence of precipitates in the form of carbides of M_6C and $M_{23}C_6$ types in Inconel 625 alloy in the joint area as the result of the normalizing.

Funding: This research was funded by The National Centre for Research and Development of Poland, grant number: DZP/M-ERA.NET-2013/2309/2014.

Conflicts of Interest: The authors declare no conflict of interest.

References

1. Karlsdóttir, S.N.; Hjaltason, S.M.; Ragnarsdóttir, K.R. Corrosion behavior of materials in hydrogen sulfide abatement system at Hellisheiði geothermal power plant. *Geothermics* **2017**, *70*, 222-229, doi:10.1016/j.geothermics.2017.06.010.
2. Tomarov, G.V.; Shipkov, A.A. Erosion–Corrosion of Metals in Multicomponent Geothermal Flows. *Therm. Eng.*+ **2006**, *53*, 188–194, doi:10.1134/S0040601506030049.
3. Koo, Y.H.; Yang, J.H.; Park, J.Y.; Kim, K.S.; Kim, H.G.; Kim, D.J.; Jung, Y.I.; Song, K.W. KAERI'S development of LWR accident tolerant fuel. *Nucl. Technol.* **2014**, *186*, 295-304, doi:10.13182/NT13-89.
4. Strasser, A.; Santucci, J.; Lindquist, K.; Yario, W.; Stern, G.; Goldstein, L.; Joseph, L. Evaluation of stainless steel cladding for use in current design LWRs. Electric Power Research Institute (Report) 1982.
5. Kosturek, R.; Wachowski, M.; Sniezek, L.; Gloc, M.; Sobczak, U. The effects of the heat treatment on the microstructure of Inconel 625/steel bimetal joint obtained by explosive welding. Proceedings of International Conference on Advanced Functional Materials and Composites (ICAFMC2018), MATEC Web of Conferences 242, Barcelona, Spain, 2018, doi: 10.1051/matecconf/201824201007.
6. EN 10216-3:2002: Seamless steel tubes for pressure purposes. Technical delivery conditions. Alloy fine grain steel tubes.
7. Farrer, J.C.M. *The Alloy Tree: A Guide to Low-Alloy Steels, Stainless Steels, and Nickel-base Alloys.*; Woodhead Publishing: England, 2004; ISBN 1-85573-766-3.
8. Pokorny, Z.; Barborak, O.; Hruby, V. Characteristics of plasma nitrided layers in deep holes. *Kovove Mater.* **2012**, *50*, 209-212, doi: 10.4149/km 2012 3 209.
9. Pokorny, Z.; Kadlec, J.; Hruby, V. Hardness of plasma nitrided layers created at different conditions. *Chem. Listy* **2011**, *105*, 717-720.
10. Pokorny, Z.; Dobrocky, D.; Kadlec, J. Influence of alloying elements on gas nitriding process of high-stressed machine parts of weapons. *Kovove Mater.* **2018**, *56*, 97-103, doi: 10.4149/km 2018 2 97.
11. Rajani, H.R.Z.; Mousavi, S.A.A.A. On Critical Criteria for Shifting Towards Plastic Strain Localization during Explosive Cladding of Inconel 625 on Low-Carbon Steel. *Combust. Explo. Shock.*+ **2013**, *49*, 2, doi:10.1134/S0010508213020172.
12. Rajani, H.R.Z.; Mousavi, S.A.A.A. The Role of Impact Energy in Failure of Explosive Cladding of Inconel 625 and Steel. *Journal of Failure Analysis and Prevention* **2012**, *12*, 6, doi:10.1007/s11668-012-9601-1.
13. Rajani, H.R.Z.; Mousavi, S.A.A.A. The effect of explosive welding parameters on metallurgical and mechanical interfacial features of Inconel 625/plain carbon steel bimetal plate, *Mater. Sci. Eng., A* **2012**, *556*, 454-464, doi:10.1016/j.msea.2012.07.012.
14. Rajani, H.R.Z.; Mousavi, S.A.A.A.; Madani, S.F. Comparison of corrosion behavior between fusion cladded and explosive cladded Inconel 625/plain carbon steel bimetal plates. *Mater. Design* **2013**, *43*, 467-474, doi:10.1016/j.matdes.2012.06.053.
15. Wachowski, M.; Gloc, M.; Ślęzak, T.; Płociński, T.; Kurzydłowski, K.J. The Effect of Heat Treatment on the Microstructure and Properties of Explosively Welded Titanium-Steel Plates. *J. Mater. Eng. Perform.* **2017**, *26*, 945-954, doi: 10.1007/s11665-017-2520-2.

16. Bristowe, W.; Pearson, M.; Stunguris, C.; Gothard, S. A Comparison of Refractory Lined Carbon Steel and Titanium EXW Clad Pressure Vessels for Specific Operating Conditions. Titanium 2010 - Proceedings of the 26th Annual Conference of the International Titanium Association, Orlando, USA, 2010.
17. Babul, T.; Oleszczak, P. Natryskiwanie powłok detonacyjnych – niektóre procesy im towarzyszące. *Inżynieria materiałowa* **2010**, *31*, 4.
18. Findik, F. Recent developments in explosive welding. *Mater. Design* **2011**, *32*, 1081-1093, doi:10.1016/j.matdes.2010.10.017.
19. Ambroziak, A. *Zgrzewanie tarciowe materiałów o różnych właściwościach*.; Wroclaw University Publishing: Poland, 2011; ISBN 978-83-7493-593-7.
20. Topolski, K.; Wieciński, P.; Szulc, Z.; Gałka, A.; Grabacz, H. Progress in the characterization of explosively joined Ti/Ni bimetals. *Mater. Design* **2014**, *63*, 479-487, doi:10.1016/j.matdes.2014.06.046.
21. Prasanthi, T.N.; Sudha, Ravikirana, C.; Saroja, S. Explosive cladding and post-weld heat treatment of mild steel and titanium. *Mater. Design* **2016**, *93*, 180–193, doi:10.1016/j.matdes.2015.12.120.
22. Kosturek, R.; Najwer, M.; Nieslony, P.; Wachowski, M. Effect of Heat Treatment on Mechanical Properties of Inconel 625/Steel P355NH Bimetal Clad Plate Manufactured by Explosive Welding, Advances in Manufacturing. *Lect. N. Mech. Eng.* **2018**, 681-686, doi:10.1007/978-3-319-68619-6_65.
23. Pocica, A.; Bański, R.; Waindok, P.; Szulc, Z.; Gałka, A. Wpływ czasu obróbki cieplnej na własności bimetalu tytan-stal. XVI Międzynarodowa Konferencja ‚Spawanie w energetyce", Opole-Jarnołtówek, Poland, 2008.
24. Jiang, H.T.; Yan, X.G.; Liu, J.X.; Duan, X.G. Effect of heat treatment on microstructure and mechanical property of Ti–steel explosive-rolling clad plate. *Trans. Nonferrous Met. Soc. China* **2014**, *24*, 697-704, doi:10.1016/S1003-6326(14)63113-7.
25. Mousavi, S.A.A.A.; Sartangi, P.F. Effect of post-weld heat treatment on the interface microstructure of explosively welded titanium–stainless steel composite. *Mater. Sci. Eng., A* **2008**, *494*, 329-336, doi:10.1016/j.msea.2008.04.032.
26. Trueb, L.F. Microstructural effects of heat treatment on the bond interface of explosively welded metals. *Metall. Trans. A* **1971**, *2*, 145–153, doi:10.1007/BF02662650.
27. Maliutina, I.; Mali, V.; Skorokhod, K.A.; Bataev, A. Effect of Heat-Treatment on the Interface Microstructure of Explosively Welded Stainless Steel – Bronze Composite. *Appl. Mech. Mater.* **2015**, *698*, 495-500, doi:10.4028/www.scientific.net/AMM.698.495.
28. Findik, F.; Yilmaz, R.; Somyurek, T. The effects of heat treatment on the microstructure and microhardness of explosive welding. *Sci. Res. Essays* **2011**, *6*, 4141-4151, doi:10.5897/SRE11.1018.
29. Fronczek, D.M.; Chulist, R.; Litynska-Dobrzynska, L.; Kac, S.; Schell, N.; Kania, Z.; Szulc, Z.; Wojewoda-Budka, J. Microstructure and kinetics of intermetallic phase growth of three-layered A1050/AZ31/A1050 clads prepared by explosive welding combined with subsequent annealing. *Mater. Design* **2017**, *130*, 120-130, doi:10.1016/j.matdes.2017.05.051.
30. Fronczek, D.M.; Chulist, R.; Szulc, Z.; Wojewoda-Budka, J. Growth kinetics of TiAl3 phase in annealed Al/Ti/Al explosively welded clads. *Mater. Lett.* **2017**, *198*, 160–163, doi:10.1016/j.matlet.2017.04.025.
31. Wang, X.G.; Li, X.G.; Yan, F.J.; Wang, C.G. Effect of heat treatment on the interfacial microstructure and properties of Cu-Al joints. *Weld. World* **2017**, *61*, 187–196, doi:10.1007/s40194-016-0393-x.
32. Chen, C.Y.; Chen, H.L.; Hwang, W.S. Influence of Interfacial Structure Development on the Fracture Mechanism and Bond Strength of Aluminum/Copper Bimetal Plate. *Metall. Trans. A* **2006**, *47*, 1232 – 1239, doi:10.2320/matertrans.47.1232.
33. Atabaki, M.M.; Nikodinovski, M.; Chenier, P.; Ma, J.; Harooni, M.; Kovacevic, R. Welding of Aluminum Alloys to Steels: An Overview. *J. Manuf. Sci. Prod.* **2014**, *14*, 59–78, doi:10.1515/jmsp-2014-0007.
34. Petrzak, P.; Kowalski, K.; Blicharski, M. Analysis of Phase Transformations in Inconel 625 Alloy during Annealing. *Acta Phys. Pol., A* **2016**, *130*, 4, doi:10.12693/APhysPolA.130.1041.
35. Shoemaker, L.E. Alloys 625 and 725: Trends in properties and applications. *Superalloys 718, 625, 706 and Derivatives* **2005**, 409-418.
36. Sukumaran, A.; Gupta, R.K.; Kumar, V.A. Effect of Heat Treatment Parameters on the Microstructure and Properties of Inconel-625 Superalloy. *J. Mater. Eng. Perform.* **2017**, *26*, 3048-3057, doi:10.1007/s11665-017-2774-8.
37. Maj, P.; Adamczyk-Cieslak, B.; Slesik, M.; Mizera, J.; Pieja, T.; Sieniawski, J.; Gancarczyk, T.; Dudek S. The Precipitation Processes and Mechanical Properties of Aged Inconel 718 Alloy After Annealing. *Arch. Metall. Mater.* **2017**, *62*, 1695-1702, doi:10.1515/amm-2017-0259.

38. Rongbin, L.; Mei, Y.; Wenchang, L.; Xianchang, H. Effects of Cold Rolling on Precipitates in Inconel 718 Alloy. *J. Mater. Eng. Perform.* **2002**, *11*, 504-508, doi:10.1361/105994902770343737.
39. Liu, W.C.; Xiao, F.R.; Yao, M.; Yuan, H.; Chen, Z.L.; Jiang, Z.Q.; Wang, S.G.; Li, W.H. Influence of cold rolling on the precipitation kinetics of γ″ and δ phases in Inconel 718 alloy. *J. Mater. Sci. Lett.* **1998**, *17*, 245-247.
40. Yunpeng, M.; Yongchang, L.; Chenxi, L.; Chong, L.; Liming, Y.; Qianying, G.; Huijun, L. Effects of cold rolling on the precipitation kinetics and the morphology evolution of intermediate phases in Inconel 718 alloy. *J. Alloys Compd.* 2015, *649*, 949-960, doi:10.1016/j.jallcom.2015.07.149.
41. López, B.; Gutiérrez, I.; Urcola, J.J. Study of the Microstructure Obtained after Diffusion Bonding Inconel 625 to Low Alloy Steel by Hot Uniaxial Pressing or Hipping. *Mater. Charact.* **1992**, *28*, 49-59, doi:10.1016/1044-5803(92)90028-G.
42. Swartzendruber, J.L.; Itkin, V.P.; Alcock C.B. The Fe-Ni (Iron-Nickel) System. *J. Phase Equilib.* **1991**, *12*, 288-312, doi:10.1007/BF02667204.